

Combining a resonance and a Raman sensor,
towards a new method for localizing
prostate tumors in vivo

Stefan Candefjord

Luleå University of Technology

Technical Report

Department of Computer Science and Electrical Engineering
Division of Media Technology

Combining a resonance and a Raman sensor, towards a new method for localizing prostate tumors *in vivo*

Feasibility Study

BIOMEDICAL ENGINEERING

Stefan Candefjord

April 12, 2007

Contents

1	Background	1
1.1	Resonance sensors	2
1.1.1	Theory	2
1.1.2	Penetration Depth	3
1.1.3	Applications	4
1.2	Raman spectroscopy	4
1.2.1	Theory	4
1.2.2	The Raman Experiment	8
1.2.3	Penetration Depth	10
2	Method, experimental setup	11
3	Expected Results	12
4	Discussion	13
5	Conclusion	14

1 Background

Cancer is a very diverse disease; a fact that complicates diagnostics and makes it hard to predict the individual clinical outcome. It will be a great challenge to be able to understand the development of different types of tumors, a more thorough knowledge would really facilitate the treatments for cancer. For example, today there exists no way to reveal a tumors potential to metastasize, and therefore no decision can be made in advance whether adjuvant therapy should be implemented or not. Despite the diversity of cancer, some common characteristics for most human tumors can be pointed out: growth is not restricted by the lack of growth signals or the presence of growth-inhibitory signals, the process of necessary death of cells (apoptosis) is prevented, new blood vessels that nourish the tumor are formed, healthy tissue is invaded and the disease spreads via metastasis. These features are all accomplished by alterations on the cellular level, such as modifications of proteins, gene or protein expression and signal transduction. Consequently, this type of information about the cancer cells can reveal the behavior of the tumor, and the progress of the cancer might then be predicted. Potentially, the treatment can even be suited for each individual. A problem today is that patients with the same type of cancer (compared using present technique) respond differently to identical treatments, the cause of this is yet unknown. The common features of human tumors also results in that the cancerous tissue exhibits macroscopical physical properties that differ from those of healthy tissue. One important characteristic is that tumors tend to be harder than healthy tissue [1]. Today, the only way to reveal a tumor *in vivo* by examining the hardness of the tissue is by means of palpation, i.e. the examiner feels the firmness of the tissue and tries to localize hard areas. Are there any other techniques that potentially can identify hard or lumpy areas in tissue *in vivo*? A new type of sensor, the resonance or tactile sensor, is a promising candidate. Tactile sensors can measure hardness, and according to *in vitro* studies they can point out cancer infected areas in tissue [1, 2]. Could they also be utilized for *in vivo* detection of tumors? If so, can a suitable complementing method that provides the critical microscopical information of the tumor be found? We think that the Raman spectrometer, which collects spectra of light that is scattered according to the Raman effect, is an excellent alternative. Our novel idea of combining the resonance and Raman techniques into one portable probe, appropriate for *in vivo* examinations, will be discussed in this paper. [3]

We will here primarily focus our attention on prostate cancer, which is the most common malignancy diagnosed in western men today [4]. Prostate cancer is an unusually difficult tumor to detect [5]. The disease is currently diagnosed first of all by measuring the amount of Prostate Specific Antigen (PSA) in the blood. PSA is synthesized only by the prostate tissue. Low concentrations of PSA are normally found in male blood. However, for men who suffer from prostate cancer the PSA level is, statistically measured, elevated. PSA is therefore contemporarily used as a marker for prostate cancer. A PSA concentration of > 4 ng/mL is considered a high level indicating that a cancer can be present. However, PSA is not a perfect marker. Clinical investigations show that many people with high levels of PSA can be healthy and vice versa, nevertheless measuring the amount of PSA is the

most widespread tool for diagnosing prostate cancer early on. If there are reasons, such as a high level of PSA or hematuria (presence of red blood cells in the urine), to suspect that someone has a tumor in the prostate a palpation is carried out to see if hard or lumpy areas in the prostate can be found. The physician feels the prostate with his fingers via the patient's rectum. A study [6] from 1991 concludes that aggressive prostate cancers are commonly palpable, whereas non-palpable tumors, often located anteromedially (located in front and toward the middle line), tend to be less aggressive. Today, palpation is looked upon as a rather crude tool [5]. To really settle that the tissue is malignant biopsies are taken and studied in microscope. Ultrasound is used to localize the prostate during the biopsy procedure. Unfortunately, ultrasound cannot direct the biopsies to spots that seem suspicious of cancer. Hence, the clinicians must take several biopsies at different locations in the prostate to assure a good chance of finding a potential cancer. 6 samples are withdrawn in the widely used sextant biopsy method, but other recommended procedures that increases the number of biopsies are more likely to detect tumors [7]. Every tissue-sample has a volume of only a thousandth of the whole prostate volume [5]. Obviously, there is a risk that a cancerous area can be overlooked and the resulting diagnose turn out false. It has been estimated that about 30% of the biopsy procedures fail to find a present cancer [8]. Moreover, the many biopsies will sometimes lead to complications, such as blood poisoning (1-7%) and hematuria (2-34%). Many patients experience severe pain during the procedure and minor complications are very common [7]. The unsatisfactory situation regarding the diagnose of prostate cancer must be improved, and a new method for the localization of tumors in the prostate is needed. [9]

1.1 Resonance sensors

1.1.1 Theory

The development of the resonance sensor, also called tactile sensor, for biomedical purposes was inspired by the clinical palpation technique [10]. Palpation is an excellent technique for observing the physical properties of living tissue, but the method cannot yield quantitative information and a good result relies on the examiner's experience [10]. The resonance sensor is able to measure the hardness of tissue, and it is useful for many applications in biomedical engineering, e.g. for determining the intraocular pressure (IOP) [1]. So how does the resonance technique work? The resonance sensor is based on the principle that the resonance frequency of a vibrating element will change when it is set in contact with a material, and the frequency shift is related to the hardness of the object. However, exactly how the frequency shift relates to the physical parameters is not yet fully understood [11]. The vibrating element can e.g. be a quartz crystal or a piezoelectric element. An advantage of the piezoelectric element is that it can be set to vibrate using a simple electrical circuit. A piezoelectric element will change its shape if exposed to an electric field (the reverse piezoelectric effect); it will therefore oscillate in response to a sinusoidal voltage variation. In other words, the piezoelectric element works as a transducer between electric and kinetic energy. This phenomenon originates from the fact that the unit cells of the

piezoelectric material behave like electric dipoles, i.e. a non-uniform charge distribution arises because the elementary cells have no center of symmetry. The resonance sensors we will use utilize ceramic piezoelectric materials, which can be pictured as composed of a mass of crystallites exhibiting dipole characteristics. Accordingly, the crystallites have non-centrosymmetric unit cells, which is true below the Curie temperature (the critical point under which the ferromagnetic state is the stable one). The Curie temperature is usually of the order of 1000 K [12]. A ceramic can be given its piezoelectric properties by applying a strong electric field over it as it is kept at a temperature near, but below, the Curie temperature. The ceramic will then be polarized in the direction of the applied field; the dipoles are locked when the field is withdrawn. The procedure will also give rise to a permanent deformation of the ceramic, as understood from the relation between polarization and mechanical stress. [1]

The principal construction of the specific type of resonance sensor that has been used in the studies [1, 2, 13], which have evaluated the tactile sensor's ability to measure intra-ocular pressure (IOP) and hardness of silicone models and prostate tissue, will now be described. The main component is a piezoelectric ceramic, made of PZT (lead, zirconate, titanate), which is driven by an electrical circuit in order to make it oscillate. The frequency at which the PZT element vibrates is monitored by a piezoelectric pick-up, which accordingly makes use of the direct piezoelectric effect – electrical polarization induced by mechanical stress. The signal from the pick-up is, after modification (only the frequency is interesting), used as feedback to the drive circuit [1]. The phase-frequency characteristics of the PZT transducer and the electronic circuits will determine which frequency the whole system will oscillate with. Incorporated into the electronics is also a phase shift circuit, whose task is to assure that the sum of the phase shifts in the complete system equals zero. When this condition is fulfilled, resonance is established. The driving frequency can in principle be arbitrarily chosen, but practically it is advantageous to maintain an oscillation frequency close to the inherent resonance frequency of the PZT element, since a high sensitivity then is prevailed. [2]

1.1.2 Penetration Depth

The resonance sensor can sense variations in hardness deep into the tissue. A good correlation between depth of a tissue layer and its contribution to tissue hardness was obtained in a recent study using an exponentially decreasing weight [2]. The impression depth of the probe affects the depth-sensing capacity; the deeper impression depth the deeper sections of the tissue can be measured [2]. The resonance sensor actually generates vibrations in the ultrasound range. For example, the particular type of resonance sensor used in a study performed by Eklund *et al.* [1], the catheter tip sensor, has a fundamental resonance frequency of approximately 200 kHz. As ultrasound propagates through tissue some of the sound energy is absorbed; there is an almost linear relationship between the absorption coefficient of tissue and the sound frequency [14]. Therefore it is reasonable to say that the penetration depth of the resonance sensor varies with the vibrational frequency of the

piezoelectric element. A transducer with a relatively low resonance frequency should be used if a large penetration depth is desired.

1.1.3 Applications

Two different applications for the resonance sensor are presented in [1, 2, 13]. Several studies in [1, 13] show that this type of sensor is suitable for measuring the intraocular pressure (IOP). An almost constant IOP (16 mmHg) is normally preserved in the eye, keeping a constant distance between cornea, lens and retina [1]. Elevated IOP increases the risk of being afflicted with glaucoma, an eye disease that is very common worldwide and a major cause of blindness today, substantially [13]. The treatment of glaucoma concentrates on lowering the IOP [13]. Consequently, the IOP is a very important parameter to monitor, and this is therefore a routine clinical examination today. The standard clinical procedure uses the Goldmann Applanation Tonometer (GAT), which measures the force exerted on a flat plate that is pressed against the cornea [14]. The Applanation Resonance Sensor (ARS) measures the frequency shift as the probe is pressed against the cornea with a constant force (the latest versions of the ARS uses the more sophisticated multipoint method, explained below). The ARS has some advantages over the GAT, e.g. is the total underestimation of the IOP in eyes that underwent corneal laser correction surgery less for ARS than for GAT [13]. Among other things the theses [1, 13] discuss the importance of the shape of the sensor tip and the development and trial of a new approach, a multipoint method continuously measuring area and force, to measure IOP. The method is based on the relation between differential change of force and area and IOP, hence it is not affected by constant terms [1]. Experiments carried out by Eklund *et al.* [1] and Jalkanen *et al.* [2] assess the tactile sensor's capability to measure hardness, in silicone models and in prostate tissue *in vitro*, and in particular to differentiate cancerous from healthy prostate tissue *in vitro*. On the basis of the findings in a recent study it is concluded that cancerous prostate tissue and healthy glandular epithelium are distinguishable using a resonance sensor [2]. But other prostate tissue types that are stiffer than the glandular epithelium, such as stroma (the supporting framework consisting of connective tissue and smooth muscle tissue) or a large concentration of prostate stones (a benign occurrence), cannot yet be told apart from tumors. However, cancer usually develops in the soft glandular tissue, of which there is a high abundance in the posterior area of the prostate [2]. Stiffness in this area can therefore be a sign of cancer. In summary, the surveys [1, 2] indicate that the prospects of detection of tumors in prostate tissue *in vivo* are good.

1.2 Raman spectroscopy

1.2.1 Theory

When a beam of light interacts with a sample, the impinging photons are scattered due to different processes. The scattered radiation can reveal much about the physical and chemical properties of the sample; an insight that has driven the development of the field

of spectroscopy. A very small part (of the order of one out of $10^6 - 10^8$) of the incident photons can, under certain circumstances, be scattered according to a special process called Raman scattering. A Raman-scattered photon will have a different wavelength than its impinging counterpart. The wavelength difference, which depends on the properties of the scattering molecule, is called a Stokes shift. From the spectrum of the Raman radiation can detailed, microscopic information about the composition of the sample be extracted. The Raman effect is named after its discoverer, the Indian professor Sir C. V. Raman, who observed the phenomenon almost 80 years ago in 1928. He was awarded the Nobel prize for the discovery already two years later. [15]

An outlined description of the complicated process of Raman scattering will now be presented. The matter subject to Raman probing is irradiated by monochromatic light, usually from a laser. As a molecule is hit by an incoming photon its electron cloud is distorted by the electromagnetic field. The photon can be treated as an oscillating dipole of the size of the wavelength of the light. This dipole is much larger than the molecule; the wavelength of visible light is 400 – 700 nm, which can be compared to the size of 0.3 – 0.4 nm for a small molecule. The electron cloud is polarized by the dipole and its geometry is thus changed; a higher state of energy is reached. This is a virtual state, which is unstable and therefore very short-lived (lasts $\sim 10^{-14}$ s). The nuclei of the molecule cannot respond to the rearrangement of electrons and establish a new position of equilibrium. Only small movements of the nuclei occur in Raman scattering, but these account for the energy differences that separate the incident and the emitted radiation. In other words, the incident photon interacts with the molecule and creates a virtual state, and almost immediately the molecule then emits a photon. The outgoing light has longer wavelength than the incident light (anti-Stokes scattering is an exception, see below), because some energy is required to move the nuclei. Remember that the nuclei of a molecule are much heavier than the electrons of their possession, and therefore the molecule's energy is greatly affected by nuclear motion. In Rayleigh scattering, which essentially is an elastic occurrence, the nuclei don't move at all during the process. It is also possible for scattered photons to gain energy as a result of the Raman process, this is called anti-Stokes scattering. Only when the molecule initially possesses abundant energy, i.e. it is in an excited energetic state, is anti-Stokes scattering enabled. At room temperature is the lowest energetic state much more densely populated than the excited states, thus anti-Stokes scattering normally only takes place to a small extent. The fact that makes Raman spectroscopy so useful is that different molecules give rise to different Stokes shifts. Hence, a Raman spectrum (ideally) contains sharp peaks that correspond to the constituents of the material. Biological tissue generally produces spectra with relatively narrow bands, typically $10 - 20 \text{ cm}^{-1}$ wide, due to the presence of many biochemicals [15]. A Raman spectrum is conventionally presented with intensity on the y-axis and the Stokes shifts, measured in cm^{-1} , on the x-axis. Stokes shifts from $3600-200 \text{ cm}^{-1}$ usually cover the information of interest. Using a laser with $\lambda = 830 \text{ nm}$ this interval corresponds to an absolute wavelength range of 844–1184 nm. A different wavelength of the laser will yield another absolute wavelength range. This also explains why a monochromatic light source of high quality is essential for obtaining sharp

Raman peaks. [16]

Which factors determine the intensity of Raman scattering? As explained, the Raman process is initiated as the electron cloud is distorted from its basic shape, which corresponds to the energetic state of the molecule, by the electromagnetic field created by the incident photon. The tendency of the electron cloud to be distorted by an electromagnetic field is termed polarizability. It is basically the polarizability of the molecule that, given a specific power and frequency of the excitation light, determines the intensity of the Raman scattering. The intensity I of the Raman scattering depends on the laser power l (assuming a laser is used as excitation light source), the frequency of the excitation light, ω , and the polarizability α according to equation 1:

$$I = Kl\alpha^2\omega^4 \quad (1)$$

where K is a constant. The Raman intensity is thus much stronger for shorter wavelengths; but observe that the Stokes shifts are not affected by a change of ω , as long as the chosen frequency still permits Raman scattering. The Stokes shifts are preserved because the energy of the virtual state is determined by the wavelength of the excitation light, but the energy difference between incident and emitted radiation is constant. The virtual state is not a real equilibrium state of the molecule, scattering (in contrast to absorption) can therefore occur regardless of whether the energy of the incident photon equals an energy gap. [16]

Can all molecules be probed by Raman spectroscopy? No, actually there are certain conditions, or selection rules, that have to be fulfilled for a molecule to be Raman active. During the lifetime of the virtual state, the nuclei of the molecule will vibrate in response to the redistribution of electrons. The selection rules follow from a quantum-mechanical treatment of the vibrations for the topical molecule. As an example, consider the vibration of a diatomic molecule. The vibration can be modeled as a harmonic oscillator, i.e. the potential energy of the nuclei as a function of displacement is a parabolic function. In this model the chemical bonding between the nuclei, which each have a mass μ , is pictured as Hookian springs with a force constant K . If the Schrödinger equation for this system is solved, eigenvalues E_v , shown in equation 2, and corresponding eigenfunctions are obtained.

$$E_v = hc\tilde{\nu} \left(v + \frac{1}{2} \right) \quad (2)$$

h is Planck's constant, c is the speed of light and $v \in \mathbb{N}_0$ is the vibrational quantum number. $\tilde{\nu} = \frac{1}{2\pi c} \sqrt{\frac{K}{\mu}}$, where K is the force constant and μ is the mass of each nucleus, is the wavenumber [cm^{-1}] of the vibration. Hence, strong bonds and light atoms will give rise to high vibrational frequencies and vice versa. Equation 2 states that the separation between two adjacent vibrational energy levels E_v and E_{v+1} is constant and equal to $hc\tilde{\nu}$, $\forall v$. This is a good approximation for the lowest energy levels, but experimentally it has been shown that as ν increases the difference between energy levels becomes smaller. The selection

rules, which not will be explained here, of quantum mechanics prohibit many vibrational transitions. For the harmonic oscillator, only transitions that fulfil $\Delta\nu = \pm 1$ are allowed. The transition $\nu = 0 \leftrightarrow 1$ produces the most intense peak in the Raman spectrum, because normally most molecules are in their lowest state of energy E_0 , where the molecule is not vibrating. [17]

Classical theory can be used to further explain some basic features of Raman scattering. Consider a diatomic molecule that is irradiated by monochromatic light with frequency ν_0 . The electrical field $E = E_0 \cos(2\pi\nu_0 t)$, where t denotes time, then induces a dipole moment $P = \alpha E = \alpha E_0 \cos(2\pi\nu_0 t)$ in the molecule. The polarizability α is a function of the nuclear displacement, because as the molecule changes shape, size or orientation the electron cloud might become easier or harder to distort. If the nuclei vibrate with a frequency ν_m , the nuclear displacement q can be expressed as $q = q_0 \cos(2\pi\nu_m t)$, where q_0 is the amplitude of the oscillation. Since $\alpha(q)$ can be regarded as a linear function of α for small amplitudes of vibration, it can be written:

$$\alpha = \alpha_0 + \left(\frac{\partial \alpha}{\partial q} \right)_0 q + \dots \quad (3)$$

where α_0 is the polarizability at $q = 0$. Substituting equation 3 into the expression for the dipole moment, and using the formula $\cos \gamma \cos \beta = \frac{1}{2} \cos(\gamma - \beta) + \frac{1}{2} \cos(\gamma + \beta)$, we obtain:

$$P = \underbrace{\alpha_0 E_0 \cos(2\pi\nu_0 t)}_{\text{Rayleigh}} + \frac{1}{2} \left(\frac{\partial \alpha}{\partial q} \right)_0 q_0 E_0 \left[\underbrace{\cos\{2\pi(\nu_0 - \nu_m)t\}}_{\text{Stokes}} + \underbrace{\cos\{2\pi(\nu_0 + \nu_m)t\}}_{\text{anti-Stokes}} \right] \quad (4)$$

The three terms in equation 4 symbolize dipoles that oscillate with frequencies ν_0 , $\nu_0 - \nu_m$ and $\nu_0 + \nu_m$. They describe Rayleigh, Stokes and anti-Stokes scattering, respectively. Note that the Stokes shift equals the vibrational frequency of the molecule, ν_m . A fundamental property of Raman scattering is understood from equation 4: if $\left(\frac{\partial \alpha}{\partial q} \right)_0 = 0$, i.e. the slope close to the equilibrium position equals zero, no Raman scattering will occur. This means that a specific vibration of a molecule is Raman active only if the pattern of atomic motions results in that the polarizability is changed during the vibrational cycle. Furthermore, since it is the slope near $q = 0$ that must equal zero, vibrations that fulfil $\left(\frac{\partial \alpha}{\partial q} \right)_0 \neq 0 \forall q \setminus \{q = 0\}$ are not Raman active. For molecules with a few atoms it can often be determined, by checking if the condition $\left(\frac{\partial \alpha}{\partial q} \right)_0 \neq 0$ is satisfied, if Raman activity is to be expected for a particular vibration. As an example two different vibrations, ν_1 and ν_3 , of the CO_2 molecule are illustrated in figure 1. The ν_1 vibration, but not the ν_3 vibration, is Raman active. For both vibrations the polarizability of the molecule is altered during the oscillatory cycle, but only for ν_1 is $\left(\frac{\partial \alpha}{\partial q} \right)_0 \neq 0$. For the ν_3 vibration the function $\alpha(q)$ shows a global minimum for $q = 0$, hence $\left(\frac{\partial \alpha}{\partial q} \right)_0 = 0$. The classical theoretical description of Raman scattering,

manifested in equation 4, also correctly predicts that the intensity of the Raman radiation generally increases as the term $\left(\frac{\partial \alpha}{\partial q}\right)_0$ becomes larger. [17]

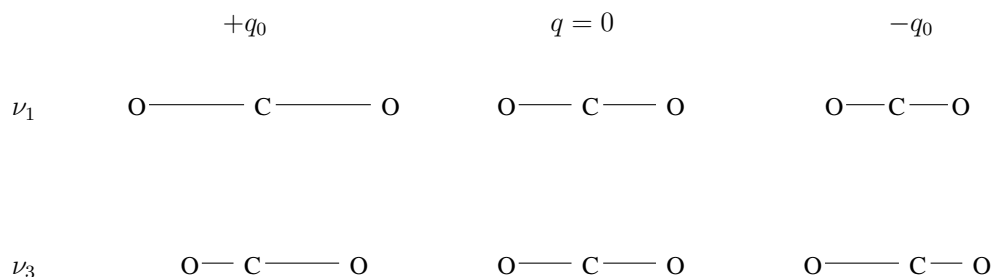


Figure 1: The ν_1 and the ν_3 vibrations of CO_2 . Only the ν_1 vibration is Raman active.

1.2.2 The Raman Experiment

Raman spectroscopy has important advantages over other spectroscopical techniques when studying biological tissue, some of which are:

1. Minimal or no preparation at all of the samples is required [16].
2. Water is a poor Raman scatterer, so the signal obtained from water does not interfere severely with the Raman spectrum [18].
3. Samples can be examined even if they are placed inside a bottle, made of e.g. glass [16].
4. As explained, the Raman spectrum is unique for each substance. The contribution that a component makes to the obtained spectrum is proportional to its relative abundance in the tissue [15]. This means that different types of tissue will give rise to different spectra.
5. Raman spectroscopy probes deep into the tissue [15]. This topic is discussed in section 1.2.3.

Unfortunately, fluorescence often interferes strongly with the Raman signal. All tissues fluoresce because they contain fluorescent chromophores, such as collagen and elastin [19]. There are different approaches to minimize the effects of fluorescence. The choice of wavelength of the excitation light is very important. Fluorescence is most problematic when the wavelength of the excitation light lies within the visible spectrum, since the fluorescence then is relatively strong and overlaps with the Raman spectrum. Utilizing a light source in the UV region fluorescence is easier to cope with; excited molecules tend to lose a great deal of the surplus energy via non-radiant processes, the fluorescence wavelength

shift then becomes much greater than the Raman shift. Thus, the spectra do not overlap that much. The fluorescence effect diminishes as the excitation light approaches the IR region. Near-IR light has too low energy to initiate most fluorescence processes. The influence of fluorescence on the final results can be reduced by subtracting a low-order polynomial, fitted to the obtained spectral curve, from the raw data. This is possible since fluorescence intensity varies slowly with the wavelength, whereas the Raman signal usually exhibits sharp peaks. The raw spectrum can also be Fourier transformed and the low-frequency components discarded. Raman microscopes can improve the ratio of the Raman and fluorescence intensities; a very small volume of the sample can be irradiated at high power, especially when confocal mode is applied [16]. [15]

To study biological tissue with good results utilizing Raman spectroscopy demands a careful choice of excitation wavelength. Due to substantial fluorescence interference the visible spectrum is not appropriate. UV excitation light could be a candidate, but UV radiation can damage tissue. Consequently, near-IR light seems to be most suitable to use. The use of excitation light with $\lambda = 830$ nm has been reported to produce little fluorescence without compromising CCD sensitivity. Wavelengths > 850 nm cannot be readily detected by a silicon based CCD. Another reason not to use longer wavelengths is that the water in the biological samples then will absorb considerably more radiation; the absorption coefficient of water increases sharply as the wavelength increases in the near-IR region [20]. [15]

A Raman probe intended for *in vivo* measurements must not require long data acquisition times to yield a high resolution. Many Raman systems are inappropriate for this reason; however, modern Raman sensors especially developed for *in vivo* use have decreased the necessary data collection time to a few seconds. Other potential problems with an *in vivo* system are probe motion artifacts and that difficulties to establish a stable probe position will lead to erroneous results. A positive observation regarding this issue was made by Shim *et al.* [21]. In their experiments the variation of pressure exerted by the probe tip on the tissue surface had no significant effect on the Raman spectra; neither had the change of angle between tip and tissue. [15]

As mentioned, a specimen's composition can be revealed by its Raman spectrum. An interpretation of an obtained spectrum can clarify the inherent constituents and their relative abundances [16]. The characteristic vibrations (interesting for Raman and infrared spectroscopy) of most common chemical groups have shown to be possible to assign approximate energy ranges that are valid for the groups in most structures [16]. Covalent bonds generally produce strong Raman signals [17]. According to [16] the spectral region from $4000\text{--}2500$ cm^{-1} is where single bonds (X-H) absorb, the interval $2500\text{--}2000$ cm^{-1} is where multiple bonds ($-\text{N}=\text{C}=\text{O}$) occur and the range $2000\text{--}1500$ cm^{-1} include the double bonds ($-\text{C}=\text{O}$, $-\text{C}=\text{N}$, $-\text{C}=\text{C}-$). The region below 1500 cm^{-1} is referred to as the Fingerprint region. Only a few groups have specific bands in this region, but many molecules exhibit complex vibrational patterns that yield unique spectral features in the Fingerprint range. Raman peaks below 650 cm^{-1} normally belong to inorganic groups,

metal-organic groups or lattice vibrations. Much effort has been put into characterizing the Raman spectra of biological materials. Carter and Edwards [18] describe, among other things, how various amide bands of protein spectra arise from the covalent linkage of the peptide bond. They discuss Raman measurements of wool, hair, nail, skin, gallstones, eyes, breast, etc. The Raman spectral characteristics of prostatic adenocarcinoma (CaP) cell lines of varying degrees of biological aggressiveness are identified and discussed in [22]. The study showed that, by means of algorithms that can differentiate the spectra despite their similar appearance, Raman spectroscopy can discriminate CaP cell lines of different degrees of malignancy. The identified Raman peaks originated from e.g. nuclear acids, DNA backbone, phospholipids, glycogen and α -helix proteins. Information of the Raman spectral features of tissue in general, and prostate tissue in particular, will be of great value for our research project.

1.2.3 Penetration Depth

The deep-sensing property of Raman measurements will substantially affect the procedure of examining the prostate tissue; this characteristic has both pros and cons. A large penetration depth can be considered advantageous because it makes it possible to sample large volumes of tissue, and the scanning of a tissue can therefore be accomplished quickly. Ideally non-invasive measurements of the prostate could be carried out if a large penetration depth is possible to attain. However, using a probe that investigates large volumes of tissue might aggravate the sensor's ability to differentiate healthy and cancerous tissue, since an obtained spectrum will be composed of spectra from a relatively large number of cells, of which only a small part might be cancerous. This problem was encountered in studies of human breast tissue; benign fibrocystic changes could not be told apart from cancerous tissue [18]. The penetration depth is dependent on the excitation wavelength [15, 19], the type of tissue that is examined [23], and actually also on the chosen modeling method and mathematical algorithm [15]. UV and visible light penetrate shallower than near-IR light (UV light of the order of microns). Unfortunately, the penetration depth of Raman measurements on tissue has not been thoroughly investigated [14, 15]. Crow *et al.* [24] declare that their probe, with $\lambda = 785$ nm, sample to a depth of 0.5 mm and a volume of 1 mm³, but they do not mention anything about under what circumstances these figures apply. In the otherwise excellent review "Prospects for *in vivo* Raman spectroscopy" by Hanlon *et al.* [15] the penetration depth in tissue for near-IR light is stated to be of the order of millimeters or centimeters (probably depending on the tissue type), detailed information has been left out. Interestingly they mention that a much larger penetration depth is achievable if problems with elastic scattering can be overcome. The design of the probe tip is critical to succeed. [15]

2 Method, experimental setup

Our final goal is to construct a portable probe that utilizes both a Raman and a resonance sensor. Since much research on detecting prostate cancer with resonance sensors currently is done by our colleagues at Umeå University, our primary task is to develop a method that, by means of a portable Ramanprobe, can discriminate prostate cancer. First of all we have to perform experiments that will aid our general understanding of Raman measurements of prostate tissue. Characteristics of the system, such as data acquisition time and penetration depth, must be determined. Sources of interference, e.g. fluorescence, will be evaluated. We will here mainly discuss what we plan to do next.

Initially, we will utilize an in-house Raman micro-spectrometer, the RENISHAW Ramascope 2000, to study prostate tissue from pigs. In particular, we want to investigate the instrument's penetration depth of the tissue. Biological tissue is highly turbid, and the process of penetration of light into the tissue is not well understood [15]. Our idea is to examine the penetration depth by placing different slices, which successively become thicker, of prostate tissue on top of a material with a known Raman spectrum – we will use plates of silicon. Silicon has a sharp Raman peak at 520 cm^{-1} [16]. If this peak can be observed when a measurement is made with the tissue-slice on top of the plate the light can penetrate through the slice. Since the prostate tissue is heterogeneous many measurements have to be performed on each tissue-slice on different spots, so that the results can be statistically evaluated. We expect that the penetration depth varies for different types of prostate tissue. For the statistical assessment it is required that at least 5-6 spots are measured 5-6 times each, more measurements can prove to be necessary to obtain a low standard deviation [25]. To bring about this experiment an instrument that can cut thin slices of tissue with great precision is needed. A microtome could perhaps be used for this purpose. A practical problem arises as these measurements are to be performed: to adjust the focus of the microscope to the surface of the silicon plate. The focus can be adjusted to the silicon plate before the tissue-slice is put in place, but since the refractive index of the biological tissue is different from that of air, the plate will no longer be in focus when the tissue is placed on top of it. A good correction is not possible to make unless the refractive index of the tissue and the distance from the plate to the lens of the microscope (of course, this can be measured) are known. Furthermore, since the prostate tissue is so complex, it is likely that the refractive index varies within the tissue and between different tissue samples. An approximative correction could perhaps be made based on the assumption that the refractive index of the prostate tissue is equal to the refractive index of water. Another idea for solving this problem is to maximize the 520 cm^{-1} Raman peak by making cyclical measurements; however, this might be very time-consuming and cumbersome, especially as the intensity of the peak decreases as thicker tissue-slices are probed.

Does the laser radiation damage the tissue? This question can be addressed by comparing spectra measured on the same spot at different times. During the experiment the tissue is constantly exposed to laser irradiation. To assure that the possible differences

between the spectra are not a consequence of dehydration it is important that the tissue is kept moist all the time; this can be done by brushing the tissue with a physiological saline solution every now and then, e.g. every fifth minute. Again, the number of measurements have to be sufficient for a statistical evaluation. In this case, the whole procedure has to be repeated several times.

If the initial experiments are successful a portable fiberoptic Raman probe will be tested. The penetration depth with this probe can be derived following a procedure analogous to the one described for the micro-Ramanprobe. We then want to compare the results, regarding similarities between spectra and the ability to penetrate into tissue, for the micro- and the portable Ramanprobe. Later on, Raman and resonance sensor trials are to be combined. Measurements with both techniques will be performed on exact same positions on prostate tissue-slices. When using the portable Ramanprobe this is easy to accomplish with a precise translational stage (the resonance sensor is also portable and can be placed next to the Ramanprobe), but with the Ramascope we need a reference mark on the specimen that functions as an origin.

To extract the full potential of the combination of the two techniques we need to employ mathematical algorithms that can help differentiating specimens. Naturally, we will start out identifying, or constructing new, algorithms suited for each one of the techniques. A mathematical model relating prostate tissue composition, hardness and frequency shift has been presented by Eklund *et al.* [1]. Jalkanen *et al.* [2] have analyzed the contribution to the measured hardness from underlying layers of tissue. Commonly used mathematical models for analyzing Raman spectra, such as principal component analysis, are discussed in [15]. Sigurdsson *et al.* [26] demonstrate a more complicated approach, they apply a neural network for diagnosis of skin cancer from Raman spectra. Subsequently, we will try to find an algorithm that compares the information obtained from each sensor; hereby, a correct diagnosis can potentially be made.

If all trials with each sensor show positive results, we will try to build one instrument that will incorporate both sensors. The Raman fiberoptic probe could maybe be cast into the piezoelectric element of the resonance sensor. The aim is to construct a portable, hand-held pen-like instrument that can be used *in vivo*.

3 Expected Results

- No studies have, to our knowledge, extensively investigated the penetration depth of Raman spectroscopy. According to [15] the penetration depth of tissue using a near-IR laser is of the order of mm–cm.
- We expect that our results will show that Raman spectroscopy can differentiate healthy and cancerous prostate tissue *in vitro*. This has been shown e.g. by Crow

et al. [24]. The overall accuracy was 86%. They used an algorithm to differentiate the specimens. *In vitro* data from a variety of studies manifest a correlation between specific Raman spectral features and disease characteristics [15].

- The combined results from the resonance and the Raman sensors will more accurately than a separate sensor differentiate cancerous and healthy prostate tissue.

4 Discussion

A combined Raman and resonance sensor has all prerequisites to be of clinical benefit for studying tissue in the seek for tumors. Both techniques have been shown to be able to differentiate tumors in human tissue *in vitro*. Raman spectroscopy has also presented promising results *in vivo* [15]. The time for a combination of the two methods is well chosen, as the development of Raman sensors using fiber optics, critical for *in vivo* measurements, now has yielded commercially available portable probes. Furthermore, the understanding and exploiting of the resonance technique has been improved during the last years [1, 2, 13]. The discussion of applications for the proposed sensor will here be limited to the diagnosis of prostate cancer. However, this technique has the potential to become a very versatile instrument, and could perhaps also be used to e.g. study breast and brain tissue as well as for applications outside the biomedical field. Another example of applications for the sensor is to identify cancerous tissue during a surgery aiming at removing a tumor, to ensure that the whole tumor, but only minimally of the healthy tissue, is taken out. We imagine that the resonance technique is to be used to scan the prostate for tissue areas suspicious of cancer. These localized spots can then be further evaluated with the Raman sensor, and a reliable diagnose can then be made. In this way, the Raman irradiation of tissue is held down. The shortcomings of the resonance sensor – it cannot yet with certainty tell if a detected hardness origins from a tumor and the localization of a potential cancer is somewhat rough – are balanced by the exactness of the Raman technique. In the future, perhaps the results will be so accurate that biopsies become unnecessary, but meanwhile biopsies will deliver the final verdict. Nevertheless, the number of biopsies can be minimized when suspicious areas are identified prior to intervention. Thus, the risk for serious complications as a result of the biopsy procedure is decreased. Furthermore, the probability that false negative results occur when taking biopsies diminishes, as the procedure now is supported by a directive guide.

We already know that the resonance sensor is a deep-sensing technique [10], even if further research must be conducted to evaluate the technique [2]. However, it is uncertain if the penetration depth of a Raman sensor is sufficient to provide non-invasive *in vivo* measurements of the prostate. An interesting alternative is to incorporate the Raman probe into a needle device, in order to protrude into the prostate with the sensor. Of course this requires that the dimensions of the probe can be made small enough to fit into the needle. The thinnest Raman probe we have come across in the literature is 2 mm thick [24]. Ac-

According to Bergh [27] the diameter of the biopsy needles used today is just below 1 mm. The biggest risk with a biopsy in the prostate is blood poisoning, since the prick is done via the rectum [27]. Bergh means that a needle with 2 mm diameter is too thick, since the risk for blood poisoning increases with the use of thick needles. Thus, an invasive Raman investigation *in vivo* is not appropriate to perform today, even though ideally only one or a few pricks would have to be done with the combined technique of our proposal. However, Raman probes can surely be made smaller in the future [15]. Awaiting the arrival of thinner probes we can evaluate invasive measuring in the prostate *in vitro* using thicker probes. It is difficult to construct thin probes because the resolution of the sensor is negatively affected when trying to shrink the diameter of the probe [28]. If invasive *in vivo* measurements can be made this would make the technique even more versatile. The penetration depth of the combined sensor must be established also for another reason: Knowledge of the penetration depth and the contributions to the measured parameters from underlying layers of tissue is necessary to localize the exact spatial position of a tumor.

The two methods complement each other. The resonance sensor gives macroscopic information about the composition of tissue, whereas the Raman sensor provides detailed microscopic information about the constituents of the tissue. A high diagnosing reliability can thus be achieved. An exemplification: If the resonance sensor has identified a hard spot in the prostate tissue, and the Raman sensor indicates that the comprising cells are cancerous, together these findings leave little doubt that a tumor has developed in the prostate.

5 Conclusion

We believe that much can be done to improve the current clinical situation regarding diagnosing prostate cancer, and we have here presented a novel idea for a device that potentially will facilitate the procedure. By means of a portable, hand-held device that combines two different sensors, tumors in the prostate are to be localized. The instrument combines a tactile sensor, which can measure hardness of the prostate tissue, with a Raman sensor that extracts information about the composition of tissue on the cellular level. Both techniques are potentially able to differentiate cancerous and healthy prostate tissue *in vivo*, promising results *in vitro* have already been presented. To rely on not only one but two sensors, with information that complement each other, can aid our understanding of the development of prostate cancer and increase the reliability of the diagnosis. Furthermore, we aim at developing efficient mathematical models that will interpret the obtained data and classify the studied tissue. This is necessary to exploit the full capacity of our sensor, especially considering that probing human tissue will yield complex data.

We will start out this project by exploring the in-house Raman spectrometer's ability to visualize the contents of prostate tissue from pigs. The reproducibility will be evaluated. One important parameter to study is the penetration depth of the method. Is it

possible to study the whole prostate non-invasively with a Raman sensor, or is the only attainable way an invasive procedure? An exact spatial localization of a tumor requires a good knowledge of the penetration depth of the combined sensor. Each of the two sensors will be studied extensively before merging them together to one unit. We hope that this project eventually will lead to a commercially available device for clinical use, and that it will increase the probabilities for a positive clinical outcome for those that suffer from prostate cancer.

References

- [1] Anders Eklund. *Resonator sensor technique for medical use - An intraocular pressure measurement system*. PhD thesis, Umeå University, Umeå, 2002.
- [2] Ville Jalkanen. Resonance sensor technology for detection of prostate cancer, 2006. Thesis (Lic). Umeå University, Umeå.
- [3] Manfred Dietel and Christine Sers. Personalized medicine and development of targeted therapies: The upcoming challenge for diagnostic molecular pathology. A review. *Virchows Arch*, 448(6):744–755, Jun 2006.
- [4] A. Razi. Prostate cancer screening, yes or no? – the current controversy. *Urology Journal*, 1(4):240–45, 2004.
- [5] A. Bergh, H. Grönberg, O. Hedestig, P. Stattin, A. Widmark, and P. Wikström. *Prostatacancer - mannens gissel*. Medicinska Fakulteten, Umeå University, 2005.
- [6] GW Baran, AL Golin, CJ Bergsma, TE Stone, PR Wilson, BA Reichardt, PF Lobert, and CS Locke. Biologic aggressiveness of palpable and nonpalpable prostate cancer: assessment with endosonography. *Radiology*, 178(1):201–206, 1991.
- [7] B Djavan, M Remzi, C C Schulman, M Marberger, and A R Zlotta. Repeat prostate biopsy: who, how and when?. a review. *Eur Urol*, 42(2):93–103, Aug 2002.
- [8] F Rabbani, N Stroumbakis, B R Kava, M S Cookson, and W R Fair. Incidence and clinical significance of false-negative sextant prostate biopsies. *J Urol*, 159(4):1247–1250, Apr 1998.
- [9] D E Neal, H Y Leung, P H Powell, F C Hamdy, and J L Donovan. Unanswered questions in screening for prostate cancer. *Eur J Cancer*, 36(10):1316–1321, Jun 2000.
- [10] S. Omata and Y. Terunuma. New tactile sensor like the human hand and its applications. *Sensors and Actuators A*, 35:9–15, 1992.
- [11] O A Lindahl and S Omata. Impression technique for the assessment of oedema: comparison with a new tactile sensor that measures physical properties of tissue. *Med Biol Eng Comput*, 33(1):27–32, Jan 1995.
- [12] F. Mandl. *Statistical Physics*. John Wiley & Sons, Chichester, 2 edition, 1988.
- [13] Per Hallberg. *Applanation Resonance Tonometry for Intraocular Pressure Measurement*. PhD thesis, Umeå University, Umeå, 2006.
- [14] Tatsuo Togawa, Toshiyo Tamura, and P. Åke Öberg. *Biomedical Transducers and Instruments*. CRC, Boca Raton, 1997.

- [15] E. B. Hanlon, R. Manoharan, T.-W. Koo, K. E. Shafer, J. T. Motz, M. Fitzmaurice, J. R. Kramer, I. Itzkan, R. R. Dasari, and M. S. Feld. TOPICAL REVIEW: Prospects for in vivo Raman spectroscopy. *Physics in Medicine and Biology*, 45:1–+, February 2000.
- [16] Even Smith and Geoffrey Dent. *Modern Raman Spectroscopy: A Practical Approach*. John Wiley & Sons, Chichester, 2005.
- [17] John R. Ferraro, Kazuo Nakamoto, and Chris W. Brown. *Introductory Raman Spectroscopy*. Academic Press, San Diego, 2 edition, 2003.
- [18] H.G.M. Edwards and E.A. Carter. Biological applications of raman spectroscopy. In Hans-Ulrich Gremlich and Bing Yan, editors, *Infrared and Raman Spectroscopy of Biological Materials*, volume 24 of *Practical Spectroscopy*, chapter 11. Marcel Dekker, New York, 2001.
- [19] B Swinson, W Jerjes, M El-Maaytah, P Norris, and C Hopper. Optical techniques in diagnosis of head and neck malignancy. *Oral Oncol*, 42(3):221–228, Mar 2006.
- [20] K. F. Palmer and D. Williams. Optical properties of water in the near infrared. *J. Opt. Soc. Am.*, 64:1107–1110, 1974.
- [21] M G Shim, L M Song, N E Marcon, and B C Wilson. In vivo near-infrared Raman spectroscopy: demonstration of feasibility during clinical gastrointestinal endoscopy. *Photochem Photobiol*, 72(1):146–150, Jul 2000.
- [22] P Crow, B Barrass, C Kendall, M Hart-Prieto, M Wright, R Persad, and N Stone. The use of raman spectroscopy to differentiate between different prostatic adenocarcinoma cell lines. *Br J Cancer*, 92(12):2166–2170, Jun 2005.
- [23] C. L. Smithpeter, A. K. Dunn, A. J. Welch, and R. Richards-Kortum. Penetration Depth Limits of In Vivo Confocal Reflectance Imaging. *Applied Optics*, 37:2749–2754, May 1998.
- [24] P Crow, A Molckovsky, N Stone, J Uff, B Wilson, and L-M WongKeeSong. Assessment of fiberoptic near-infrared raman spectroscopy for diagnosis of bladder and prostate cancer. *Urology*, 65(6):1126–1130, Jun 2005.
- [25] Olof Lindahl (private communication).
- [26] Sigurdur Sigurdsson, Peter Alshede Philipsen, Lars Kai Hansen, Jan Larsen, Monika Gniadecka, and Hans Christian Wulf. Detection of skin cancer by classification of Raman spectra. *IEEE Trans Biomed Eng*, 51(10):1784–1793, Oct 2004.
- [27] Anders Bergh (private communication).
- [28] Kerstin Ramser (private communication).